American Mineralogist, Volume 72, pages 299–311, 1987

Crystal-growth kinetics of plagioclase in igneous systems: One-atmosphere experiments and application of a simplified growth model

Gregory E. Muncill
Geophysical Laboratory, 2801 Upton Street, N.W., Washington, D.C. 20008, U.S.A.
Antonio C. Lasaga
Department of Geology and Geophysics, Yale University, New Haven, Connecticut 06511, U.S.A.

ABSTRACT

Crystal-growth rates have been determined experimentally at 1 atm for the growth of plagioclase from selected compositions (An_{10-40}) of the albite-anorthite melt system. The growth-rate data from the present study, when combined with the previous results of Kirkpatrick et al. (1979), can be described by an extension of simple, single-component growth theory to multicomponent systems as proposed by Lasaga (1982).

The observed experimental growth rates can be combined with data on compositional gradients in crystals and glass (quenched melt) in order to place limits on possible kinetic models of crystal growth. Growth rates at small undercoolings ($\Delta T = T_{\text{Liquidus}} - T_{\text{Growth}} \leq$ 20 deg C) appear to be controlled by crystal-melt interface kinetics, and growth is linear with respect to time. At moderate undercooling (20 deg $\leq \Delta T \leq$ 80 deg), there are a few possible models; the rate-controlling step may be either a steady-state (time-independent) process or a slow approach toward equilibrium during crystal growth. In either case, at moderate undercoolings the experimentally observed growth rates of plagioclase for a particular bulk composition are likely to be slower than the theoretically predicted growth rate because of mass-transport (diffusion) effects. At large undercoolings ($\Delta T \geq$ 80 deg), growth is controlled by diffusive mass transport, and growth rates are nonlinear with respect to time.

INTRODUCTION

Over the past several decades, a majority of experimental investigations in experimental igneous petrology have been concerned with magmas at equilibrium. Although much more work is still required, a substantial foundation has been developed for describing igneous systems at thermodynamic equilibrium. These equilibrium models are not path dependent and thus represent time-independent processes. Many natural igneous rocks, however, contain abundant geochemical evidence of disequilibrium, such as compositional zoning in minerals and the nonapplicability of the phase rule for a particular mineral assemblage. The magmas from which these rocks formed must have followed a nonequilibrium, time-dependent pathway that is recorded in the disequilibrium geochemical features and the petrographic texture of the rock. The challenge for igneous petrologists is the interpretation of the time-dependent evolution of these igneous systems from the geochemical and textural data.

An understanding of kinetic-related features in igneous rocks requires detailed models of reactions in igneous systems. Unfortunately, kinetic theory concerning rates of crystal growth or rates of partial melting in igneous systems is still in an initial state of development (Kirkpatrick, 1981). Detailed studies of crystal growth and dissolution in silicate melts are of critical importance for developing molecular models of igneous reaction kinetics. With the ultimate development of molecular models, it will be possible to decipher and model the particular kinetic pathway of a natural system from geochemical and petrographic records preserved in the rocks.

The present experimental study was undertaken to investigate crystal growth in a simple, but very important, silicate melt system. Growth rate and compositional data can be used to evaluate current theoretical models of crystal growth. In particular, results of the present study can be used to test extensions of simple, single-component growth models to multicomponent systems.

The plagioclase (albite-anorthite) melt system was chosen for this study for the following reasons: (1) plagioclase is a ubiquitous igneous mineral, (2) plagioclase exhibits complex compositional zoning, which may be related to the kinetics of plagioclase crystal growth, and (3) the phase equilibria of the simple system, which delineate regions of zero overall reaction rates, are relatively well known. Crystal growth in the 1-atm system has been previously investigated by Kirkpatrick et al. (1979), although a majority of their data are for the bulk compositional range of An_{50}–An_{100}. For the present investigation, crystal-growth rates were determined for melts within the bulk compo-

0003–004X/87/0304–0299$02.00

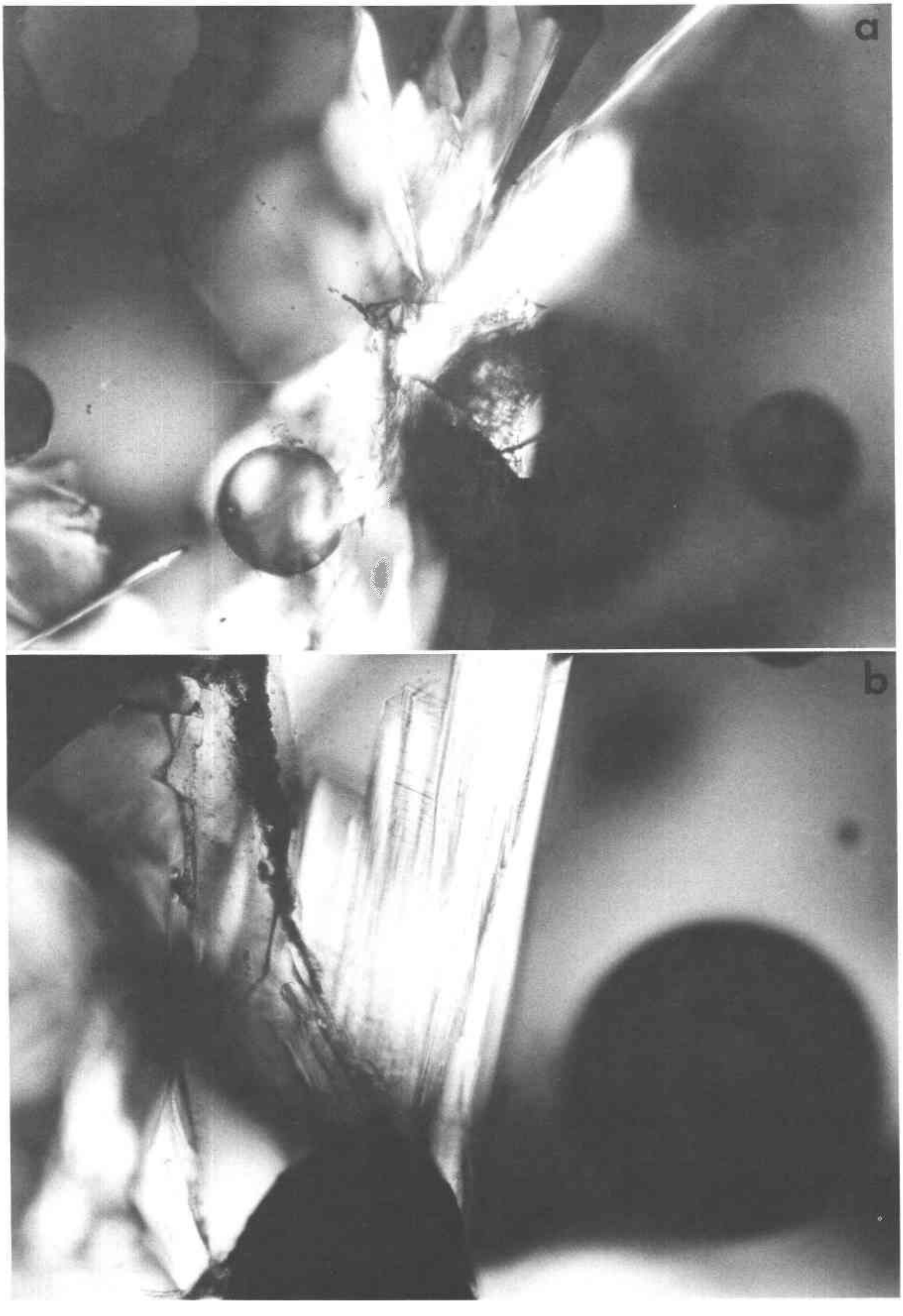
a
b

TABLE 1. Nominal and analyzed compositions of starting materials

	An-10*		An-20*		An-30*		An-40*		Anorthite seed analyzed‡
Oxide	Nominal	Analyzed	Nominal	Analyzed	Nominal	Analyzed	Nominal	Analyzed	
SiO_2	66.0	65.0	63.4	62.5	60.8	59.8	58.2	57.9	45.5
Al_2O_3	21.3	21.6	23.1	23.2	24.8	25.6	26.6	27.2	35.1
CaO	2.1	2.2	4.2	4.2	6.3	6.1	8.4	8.2	19.6
Na_2O	10.6	10.5	9.3	9.4	8.1	8.3	6.9	7.0	0.8
L.O.I.†		0.3		0.8		0.4		0.4	
Total	100.0	99.6	100.0	100.1	100.0	100.2	100.1	100.7	101.0
				Cations on the basis of eight oxygens					
Si	2.90	2.88	2.80	2.78	2.70	2.67	2.60	2.58	2.08
Al	1.10	1.13	1.20	1.21	1.30	1.35	1.40	1.43	1.89
Ca	0.10	0.10	0.20	0.20	0.30	0.29	0.40	0.39	0.96
Na	0.90	0.90	0.80	0.81	0.70	0.72	0.60	0.61	0.07
Total	5.00	5.01	5.00	5.01	5.00	5.02	5.00	5.01	5.01

* Wet-chemical analysis.
† Loss on ignition.
‡ Average of 10 spot analyses with an electron-microprobe analyzer.

sitional range An_{10}–An_{40}. The compositions of plagioclase crystals that grow from melts within this bulk compositional range are similar to compositions of naturally occurring, complexly zoned plagioclase crystals from a variety of rock types (Vance, 1962). Thus, proposed kinetic models for the origins of geochemical features such as oscillatory zoning in plagioclase (Sibley et al., 1976; Haase et al., 1980; Allegre et al., 1981) can ultimately be tested.

EXPERIMENTAL PROCEDURE

Preparation of starting materials

The compositions of the anhydrous starting materials correspond to plagioclase compositions of An_{40}, An_{30}, An_{20}, and An_{10}. The starting materials were prepared as gels (Luth and Ingamells, 1965). The gels were dried in an oven at 120°C for 12 h and were subsequently fired in stages at temperatures from 400 to 950°C. The resulting sintered mixtures were ground in an agate mortar and pestle in order to pass through a #200 mesh sieve. The nominal compositions and wet-chemical analyses are presented in Table 1.

In order to confine the present study to an investigation of crystal growth, it was necessary to separate the effects of crystal growth from the effects of nucleation. A majority of previous experimental studies have included the added complication of homogeneous nucleation, with a resulting lack of accuracy in determining the time of initiation of crystal growth. The present investigation avoided the "added variable" of nucleation through the use of seed crystals. Seed crystals of uniform size (100–250 μm) were prepared from crystals of natural, igneous anorthite (An_{97}) by grinding and sieving. An average of several electron-microprobe analyses of seed crystals is presented in Table 1.

One-atmosphere experiments

Crystal-growth experiments were performed at 1 atm in a vertical-tube quench furnace. The experimental charges were prepared by mixing 150 mg of the appropriate starting composition with approximately 1 mg of seed crystals. The mix was placed into a 5-mm-diameter Pt capsule that had been welded shut at one end. The experimental charge was suspended next to a Pt-$Pt_{90}Rh_{10}$ thermocouple in the vertical-tube furnace. All charges were initially brought to a temperature 30 deg above the appropriate liquidus temperature for a period of 25 min to 2½ h. It was found by trial and error that 30 min was the optimum homogenization time for melting of the An_{40} bulk composition, because longer times resulted in substantial dissolution of the anorthite seed crystals. Longer homogenization times were used with more albite-rich An_{10} and An_{20} bulk compositions because the seed crystals did not dissolve as readily into these more viscous melts. The formation of compositional gradients in the melt next to the seed crystals from dissolution effects was checked by "zero-time" studies of runs quenched immediately after homogenization. There were no detectable compositional gradients in the glasses surrounding the seed crystals.

In the first set of experiments, the temperature of each run was decreased from the homogenization temperature to the appropriate growth temperature by adjusting the temperature controller. Owing to thermal inertia of the furnace, it took up to several minutes to reach some of the lower run temperatures, and temperature undershooting was a common phenomenon. Kirkpatrick et al. (1979) noted that similar growth rates could be obtained from experiments on supercooled melts and experiments employing reheated glasses (quenched melt). From preliminary runs during the present study, no differences were observed in results from crystal-growth experiments with supercooled melts or reheated quenched glasses. Therefore, most of the present 1-atm experiments were conducted with quenched glasses.

The 1-atm crystal-growth experiments with quenched glasses were carried out by inserting the experimental charge in the vertical-tube furnace at the appropriate crystal-growth temperature. In all cases, the reading thermocouple approached the run temperature within 1.5 to 2 min. Although there may have been a

←

Fig. 1. Photomicrographs of plagioclase crystal morphology. (a) Crossed polars of thin, tabular crystals radiating from an anorthite nucleus. The field of view is 0.8 mm across (long edge). $\Delta T = 18$ deg, $c = An_{30}$. (b) Crossed polars of crystals with skeletal morphology. The field of view is 0.8 mm across. $\Delta T = 37$ deg, $c = An_{40}$.

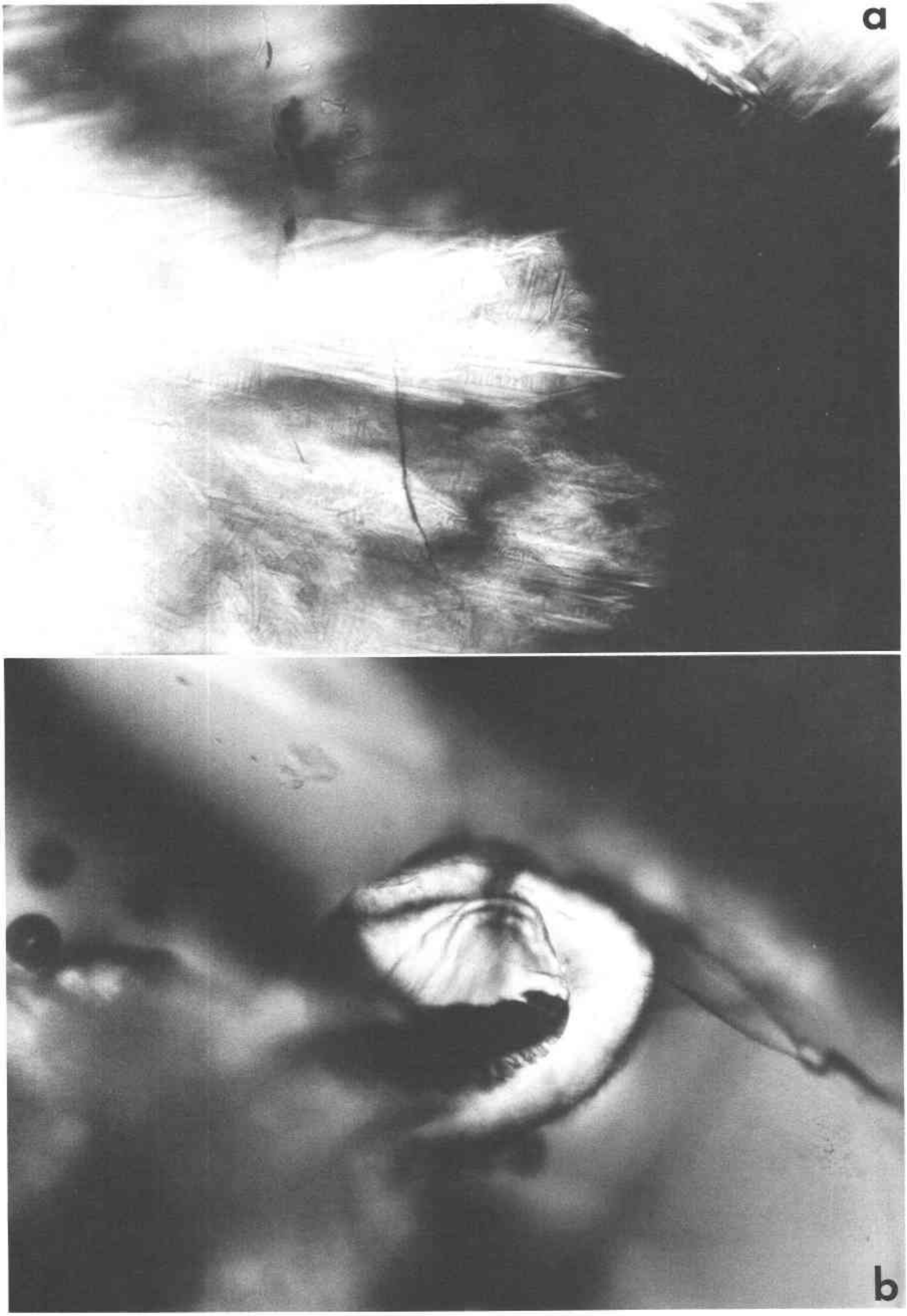
a
b

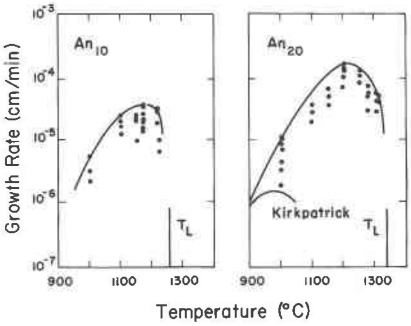

Fig. 3. Plots of crystal-growth rates vs. temperature for An_{10} and An_{20} bulk compositions.

slower rise time associated with the experimental charge, the time required to reach thermal equilibrium according to heat-flow calculations is less than 2 to 3 min, which is significantly less than the time required to bring runs from superliquidus melt temperatures to the growth temperatures. Each experiment was quenched in a stream of air. The capsule would quench to below red heat within 2 to 4 s. The run products were mounted in epoxy, and a polished thin section was produced from the epoxy block. The polished thin sections were investigated with the aid of an optical microscope and an electron-microprobe analyzer in order to determine optical and chemical properties of the plagioclase crystals.

EXPERIMENTAL RESULTS

Crystal morphologies

For all of the compositions (An_{10}, An_{20}, An_{30}, An_{40}), there was a progressive change of crystal morphology with degree of undercooling, as has been noted previously by Kirkpatrick et al. (1979). At undercoolings of less than 40 deg, plagioclase occurs as euhedral, faceted crystals that appear as thin platelets (see Fig. 1a). The crystals have an average aspect ratio (*a*:*b*:*c*) of 20:1:20, as determined by optical methods. Thus, the crystals are tabular, with the largest growth face (in area) being represented by the {010} face. This observation is in general agreement with the predominant morphology of natural plagioclase crystals (Heinrich, 1965; Deer et al., 1966), although natural crystals have significantly smaller aspect ratios than those of the synthetic crystals.

At undercoolings of 40 to 60 deg, the resulting crystals are skeletal; this morphology is even the case for the crystal overgrowths around the anorthite seed crystals (see Fig. 1b). The average *a*:*b*:*c* aspect ratio of these crystals is approximately 25:1:5. The **a** axis is the direction of principal growth, which has been observed in other feldspar-crystallization studies (Fenn, 1977; Swanson, 1977) and is common in nature (Deer et al., 1966). the only experimental variation to this pattern is the anorthite crystal-growth study of Klein and Uhlmann (1974), in which the anorthite was reported to be elongate along the **c** axis.

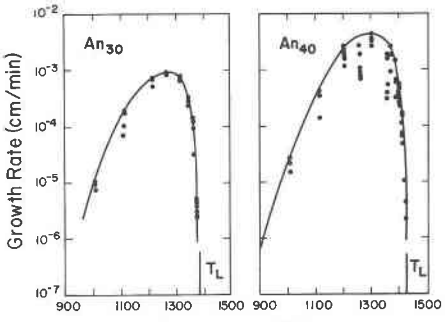

Fig. 4. Plots of crystal-growth rates vs. temperature for An_{30} and An_{40} bulk compositions.

At undercoolings of 60 to 80 deg, the crystals form dendrites (see Fig. 2a), with side branches growing from the major dendrite arms. The crystallographic direction of primary growth cannot be determined by conoscopic optical methods, because of the small size of the dendrites. The length-fast character of the dendrites precludes the **b** crystallographic axis as the principal growth direction, but no distinction can be made as to whether the **a** or **c** axis is the predominate elongate crystallographic axis.

At undercoolings greater than 80 deg, the crystal form of the plagioclase surrounding the seed crystals is spherulitic or fibrillar (see Fig. 2b). Many of the very fine plagioclase needles do, however, maintain faceted shapes at the tips of the crystals. In addition, as noted by Kirkpatrick (1981) for other systems, the thickness of the crystals and the spacing between crystals within the bundles or spherules decrease with increased undercooling.

When observed optically under crossed polars, the crystals appear to be unzoned, because there is no change in extinction angle within the individual crystals. Many of the individual crystals also contain growth twins; this phenomenon was observed primarily in crystals that grew at uncercoolings of less than 60 deg.

Growth rates

The crystal-growth data have been plotted versus temperature, a common method for presentation of growth data (Kirkpatrick, 1981), for each of the compositions (Figs. 3 and 4). The "best fit" lines were hand-fit to the maxima of the growth data for each growth temperature that was investigated. One reason for the scatter in the

←

Fig. 2. Photomicrographs of plagioclase crystal morphology. (a) Crossed polars of dendritic crystals. The field of view is 0.32 mm across. $\Delta T = 60$ deg, $c = An_{40}$. (b) Spherulitic morphology of crystals around a seed crystal as viewed through crossed polars. The field of view is 0.8 mm across. $\Delta T = 123$ deg, $c = An_{40}$.

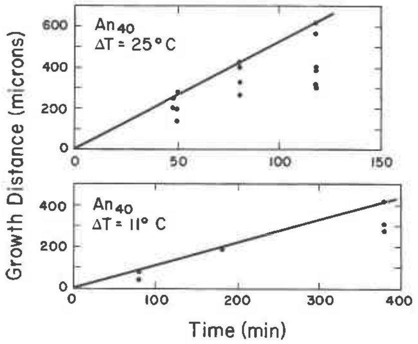

Fig. 5. Plots of crystal lengths vs. time for small undercoolings.

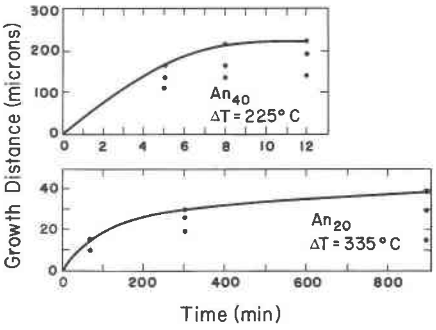

Fig. 6. Plots of crystal lengths vs. time for large undercoolings.

growth-rate data is related to the orientations or "cuts" of the measured crystals. For each measured crystal, the maximum lengths were measured from the edge of the seed crystal to the edge of the overgrowth crystal along the elongated direction. The length of this measurement can vary as a function of crystal orientation and cut of the thin section. In addition, growth can be inhibited by crystal impingement, which is not always observable in the nearly two-dimensional thin section. Finally, as shown later, crystal-growth rates at large undercoolings are not constant with respect to time. For the present study, primary interest is in *initial* growth rates, before chemical diffusion in the melt becomes a rate-limiting step. Thus, the operating assumption in using the growth-rate data is that the maximum growth rates for each temperature represent "true" growth rates or growth in the absence of compositional gradients in the melt.

The growth-rate curves are similar in form to those found for other glass-forming materials (Winkler, 1947; Jackson, 1967; Kirkpatrick et al., 1967). The growth rate initially increases with undercooling below the liquidus, passes through a maximum, and finally decreases with further undercooling.

The development of time-independent growth rates, which represent linear growth kinetics, have important implications for possible growth mechanisms (Kirkpatrick et al., 1979). Therefore, the applicability of time-independent growth rates was tested by performing time-distance experiments with An_{40} and An_{20} bulk compositions. Isothermal crystal-growth experiments were performed for varying lengths of time, and the corresponding crystal lengths were plotted versus time. The results, plotted in Figures 5 and 6, show that for relatively small undercoolings, the growth kinetics are linear. For relatively large undercoolings, however, the crystals do *not* grow in a linear fashion with respect to time. For comparison, Kirkpatrick et al. (1979) found that the growth rates for An_{50} and An_{75} bulk compositions were independent of time, even for large undercoolings. Possible reasons for the differences in the present experiments and those of Kirkpatrick et al. will be discussed later.

DISCUSSION

General theory of growth from a melt

Rates of crystal growth can be "controlled" by any of three principal processes: (1) interfacial kinetics or the rate of attachment at the crystal face, (2) transport of material by diffusion or a combination of diffusion and advection through the melt phase, and (3) transport of latent heat of crystallization away from the crystal face. Although only one process may be the dominant rate-controlling step under one set of conditions or at any one time, there may be transition regions where combinations of processes dominate. For crystallization in multicomponent, silicate melt systems, the transport of heat away from the crystal face will be rapid relative to chemical transport in the melt (Bottinga et al., 1966). Thus, the primary concern will be determining the interplay between interfacial reaction kinetics and diffusive transport through the melt as rate-controlling processes.

If the interface reaction is the rate-controlling step in the crystal-growth process, a simplified general theory that treats crystal growth as an elementary activated process has been developed for modeling crystal growth (Turnbull and Cohen, 1960; Jackson, 1967). The theoretically derived, growth-rate law for a single-component system is of the form

$$Y = [1 - \exp(-\Delta H_m \Delta T/RTT_L)]Y_r/\eta, \quad (1)$$

where Y = growth rate (cm/s), ΔH_m = enthalpy of melting (J/mol), R = gas constant (J/K·mol), T = temperature of growth (K); T_L = liquidus temperature of the crystalline phase (K), $\Delta T = T_L - T$ (K), Y_r = reduced growth rate (cm·poise/s·K), and η = viscosity of the melt phase (poise). A particularly important aspect of Equation 1 is that the diffusion of growth units through the melt toward the crystal-melt interface is assumed to follow a Stokes-Einstein relationship:

$$D(T) = kT/3\pi a_0 \eta(T), \quad (2)$$

where $\eta(T)$ = viscosity (which will be temperature dependent), a_0 = diameter of the diffusing species, and k = Boltzmann's constant.

In the Stokes-Einstein model, the diffusion coefficient,

TABLE 2. Values of *A* coefficients for polynomial expression of the 1-atm liquidus curve for the plagioclase system

A	Value	*A*	Value
0	1 099.401 738 69	5	653 438.497 314
1	2 821.457 311 03	6	−916 859.113 281
2	−18 352.213 684 1	7	794 534.039 062
3	90 523.445 922 9	8	−385 967.648 682
4	−299 952.079 346	9	80 267.177 2461

D, is proportional to the inverse of the viscosity, η, of the melt phase. The reduced growth rate, Y_r, incorporates all of the factors left after the simplifications of the fundamental theory. Basic terms represented in Y_r include the fraction of sites on the crystal surface available for attachment of growth units, a function that incorporates the dynamics of attachment and all of the terms from the Stokes-Einstein relationship except viscosity (Kirkpatrick, 1975).

Although the basic theory was originally developed for crystal growth in single-component systems, it can be adapted for multicomponent systems with a few additional assumptions. The following formulation was originally developed by Lasaga (1982) as an application of a master equation of crystal growth. For growth in an anhydrous binary system, such as the plagioclase melt system at 1 atm, Equation 1 will still be valid for interfacial-controlled growth. Furthermore, the assumption will be made that the growth mechanism and the Stokes-Einstein terms are similar for the entire plagioclase system; the reduced growth rate, Y_r is, therefore, independent of composition over the compositional range of the plagioclase system. Data are available for growth rates in the single-component anorthite system as a function of undercooling (Kirkpatrick et al., 1976), which can be fit to a polynomial of ΔT:

$$Y_{\mathrm{An}}\eta/\Delta T = (3.548 \times 10^{-5})\Delta T + (3.833 \times 10^{-8})\Delta T^2 + (6.372 \times 10^{-9})\Delta T^3. \quad (\mathrm{cm \cdot poise/s \cdot K}) \quad (3)$$

For small ΔT values, Equation 1 can be expanded for the growth of anorthite in the single-component system to yield

$$Y_{\mathrm{An}} \simeq (\Delta H_{\mathrm{m,An}}\Delta T/\eta_{\mathrm{An}} T T_{\mathrm{m,An}} R) Y_r. \quad (\mathrm{cm/s}) \quad (4)$$

With small ΔT values, there will be the approximation $T \approx T_{\mathrm{m,An}}$, and if $\Delta H_{\mathrm{m,An}}$ is assumed to be independent of temperature, Equation 4 can be further simplified to

$$Y_{\mathrm{An}} \simeq (\Delta H_{\mathrm{m,An}}\Delta T/\eta_{\mathrm{An}} R T^2_{\mathrm{m,An}}) Y_r \quad (\mathrm{cm/s}) \quad (5)$$

or

$$\frac{Y_{\mathrm{An}}\eta_{\mathrm{An}}}{\Delta T} = \left(\frac{\Delta H_{\mathrm{m,An}}}{R T^2_{\mathrm{m,An}}}\right) Y_r$$
$$= (3.548 \times 10^{-5})\Delta T + (3.833 \times 10^{-8})\Delta T^2 + (6.372 \times 10^{-9})\Delta T^3. \quad (\mathrm{cm \cdot poise/s \cdot K}) \quad (6)$$

Solving for Y_r and substituting into the general equation (Eq. 1) yields

$$Y_{\mathrm{Pl}} = \left[1 - \exp\left(\frac{-\Delta H_{\mathrm{m,Pl}}\Delta T}{R T^2_{\mathrm{m,An}}}\right)\right]\left(\frac{R T^2_{\mathrm{m,An}}}{\Delta H_{\mathrm{m,An}}\eta_{\mathrm{Pl}}}\right) \cdot [(3.548 \times 10^{-5})\Delta T + (3.833 \times 10^{-8})\Delta T^2 + (6.372 \times 10^{-9})\Delta T^3], \quad (\mathrm{cm/s}) \quad (7)$$

where Y_{Pl} = growth rate of plagioclase of composition Pl, $T_{\mathrm{m,An}}$ = melting temperature of pure anorthite (1830 K), $\Delta H_{\mathrm{m,Pl}}$ = enthalpy of melting of plagioclase of composition Pl (J/mol), $\Delta H_{\mathrm{m,An}}$ = enthalpy of melting of anorthite (J/mol), η_{Pl} = viscosity of the plagioclase melt of composition, Pl at the temperature of growth (poise), T = growth temperature for the system (K), T_{L} = liquidus temperature for the particular binary composition (K), and $\Delta T = T_{\mathrm{L}} - T$ (K).

In order to model growth as a function of concentration, $Y(c)$, the values of T_{L}, ΔH_{m}, and η are required as functions of the melt composition. Because we will be assuming local equilibrium, the pertinent melt composition is the appropriate composition at the crystal-melt interface [$c(0,t)$].

The liquidus temperature, T_{L}, can be found as a function of c by fitting the data of Bowen (1913) to a polynomial of the anorthite mole fraction, c, as shown by

$$T_{\mathrm{L}} = \sum_{n=0}^{9} A_n c^n, \quad (^\circ\mathrm{C}) \quad (8)$$

where the A constants are given in Table 2. This expression reproduces the liquidus curve for the 1-atm plagioclase system to within ±2 deg.

The viscosity was originally modeled by Lasaga (1982) according to the empirical equations of Bottinga and Weill (1972). More recently, viscosities have been measured for

TABLE 3. Values of *B* coefficients for polynomial expression of the 1-atm viscosity of a plagioclase melt

i	*j* = 0	*j* = 1	*j* = 2	*j* = 3
0	61.022 907 3	−0.107 498 452	$7.376\,719\,44 \times 10^{-5}$	$-1.81\,892\,95 \times 10^{-8}$
1	0.180 493 176	−3.854 200 19	$1.597\,349\,52 \times 10^{-7}$	
2	$6.810\,228\,23 \times 10^{-4}$	$-4.093\,598\,7 \times 10^{-7}$		
3	$5.720\,620\,49 \times 10^{-7}$			

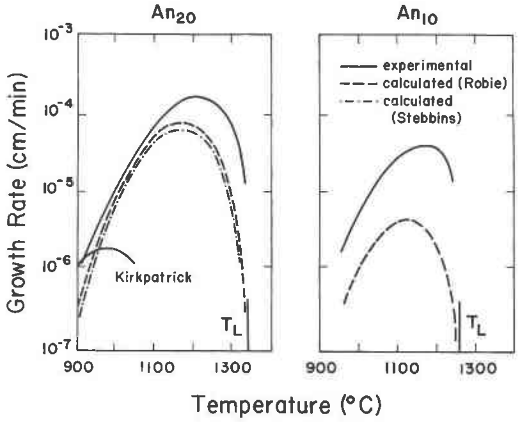

Fig. 7. Plots of experimental and calculated curves of crystal-growth rates vs. temperature for An_{10} and An_{20} bulk compositions. The data of Kirkpatrick et al. (1979) are shown for comparison. Calculated curves were constructed from the data of Robie et al. (1978) and Stebbins et al. (1983).

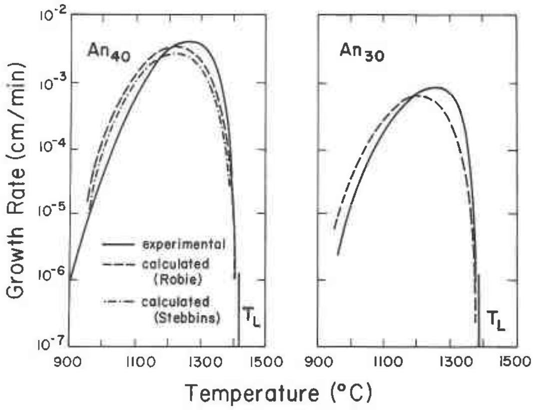

Fig. 8. Plots of experimental and calculated curves of crystal-growth rates vs. temperature for An_{30} and An_{40} bulk compositions. Calculated curves were constructed from the data of Robie et al. (1978) and Stebbins et al. (1983).

the plagioclase melt system by Cranmer and Uhlmann (1981). Although their data appear to fit Bottinga and Weill's curves at relatively high anorthite contents ($c \geq 0.5$), their measured viscosities for more albitic compositions ($0 \leq c \leq 0.2$) are up to 1.5 orders of magnitude larger than Bottinga and Weill's predicted viscosities. Cranmer and Uhlmann apparently did not recognize the inconsistency because of an error in either calculating or plotting curves from Bottinga and Weill's empirical model. For this reason, the data of Cranmer and Uhlmann have been fitted to a surface in composition-temperature space through the use of a linear, least-squares technique. The resulting mixed third-degree polynomial is obtained after the method of Goodman (1983) as

$$\log_{10}\eta = \sum_{i=0}^{3} \sum_{j=0}^{3-i} B_{ij}T^jC^i_{An}, \qquad (9)$$

where T is temperature in °C, C_{An} is the anorthite content of the melt in *mole percent,* and the B_{ij} constants are as given in Table 3. This viscosity equation reproduces viscosities to within 0.2 log units of Cranmer and Uhlmann's experimental values for a wide temperature range (850–1600°C) and the complete anhydrous plagioclase compositional range.

The appropriate ΔH_m for crystal growth in the plagioclase system will correspond to the reaction

$$An_{m,c} \rightarrow yAn_{m,0} + (1 - y)An_{s,q}. \qquad (10)$$

One mole of plagioclase melt of composition c (c = concentration of the anorthite component) is used to produce $(1 - y)$ moles of plagioclase crystal with a composition of q. Because of the crystal-liquid partitioning, all of the anorthite component of the melt is used in the reaction, and y moles of albite component ($c = 0$) is left in the melt. From mass-balance considerations, it also follows that

$$c = y \cdot 0 + (1 - y)q, \qquad (11)$$

which can be rearranged as

$$y = (q - c)/q. \qquad (12)$$

If ideal mixing of components in the crystalline and melt phases is assumed, which is probably an adequate estimate for the high temperatures of the growth experiments, the enthalpy of melting, which corresponds to the reverse of Reaction 10, can be written as

$$\begin{aligned}\Delta H_{m,An_q} = {} & cH^0_{m,An} + (1 - c)H^0_{m,Ab} - yH^0_{m,Ab} \\ & - (1 - y)(qH^0_{s,An} + (1 - q)H^0_{s,Ab}), \end{aligned} \qquad (13)$$

where $\Delta H_{m,An_q}$ = enthalpy of melting of plagioclase of composition q and $H^0_{z,x}$ = enthalpy of phase z of pure composition x at 1 bar and T. Substituting for c from Equation 12, results in

$$\begin{aligned}\Delta H_{m,An_q} = {} & (1 - y)q(H^0_{m,An} - H^0_{s,An}) \\ & + (1 - y)(1 - q)(H^0_{m,Ab} - H^0_{s,Ab}) \end{aligned} \qquad (14)$$

or

$$\Delta H_{m,An_q} = c[q\Delta H_{m,An} + (1 - q)\Delta H_{m,Ab}]/q. \qquad (15)$$

Finally, the assumption of local equilibrium between the crystal and melt phases results in

$$K = q/c, \qquad (16)$$

where K is the equilibrium partition coefficient. Substituting for q in Equation 15 from Equation 16 yields

$$\Delta H_m = c\Delta H^m_{An} + [(1 - Kc)/K]\Delta H^m_{Ab}. \qquad (17)$$

The required information now has been accumulated to calculate, through the use of the general equation (Eq. 7), the growth rates for plagioclase in the binary system solely from growth data on an endmember composition (An_{100}).

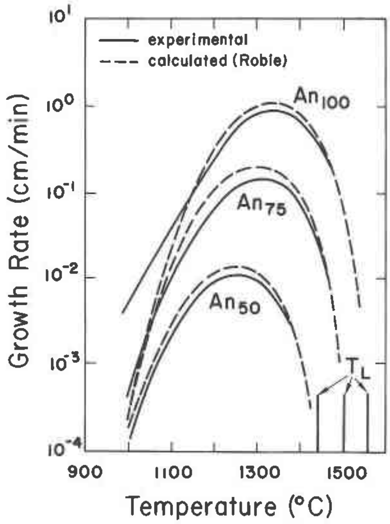

Fig. 9. Plots of experimental growth rates of Kirkpatrick et al. (1979) compared with calculated curves from the present study.

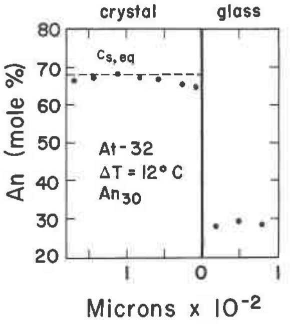

Fig. 10. Compositions of crystal and glass for run At-32.

Comparison of simple theory with 1-atm experiments

Lasaga (1982) developed the general equation (Eq. 7) in order to model crystal growth across the entire plagioclase compositional range. Although Lasaga's calculated curves fit the experimental data of Kirkpatrick et al. (1979) reasonably well for anorthite-rich compositions ($c \geq 0.5$), the calculated curve was a poor fit to the albite-rich composition ($c = 0.2$).

Equation 7 was used, in combination with the newly derived viscosity relationships, to calculate growth rates for the compositional range of the present investigation and the more anorthite-rich compositions investigated by Kirkpatrick et al. (1979). The values used for $\Delta H_{m,An}$ and $\Delta H_{m,Ab}$ were 81 000 and 59 000 J/mol, respectively (Robie et al., 1978). Although there still remains considerable controversy concerning the value of $\Delta H_{m,An}$, it will be shown that Equation 7 is relatively insensitive to moderate changes in the ΔH_m values.

The calculated versus experimental curves for the compositions of the present study are plotted in Figures 7 and 8. Calculated versus experimental curves are plotted in Figure 9 for the experimental data of Kirkpatrick et al. (1979). In addition, growth rate versus temperature curves were calculated from Equation 7 for crystal growth from An_{40} and An_{20} bulk compositions with the recommended ΔH_m values of Stebbins et al. (1983) ($\Delta H_{m,An} = 136\,000$ and $\Delta H_{m,Ab} = 63\,000$ J/mol). The resulting curves are nearly identical to the curves calculated from the data of Robie et al. (1978). Calculated curves for the other bulk compositions employing the data of Stebbins et al. (1983) are not shown, but the agreement is similar.

In general, there is close agreement between the calculated and experimental curves for the relatively anorthite-rich bulk compositions, with the primary difference consisting of a shift in the growth-rate maxima to lower temperatures (increased undercooling) for the calculated curves as compared to the experimental curves. In a comparison of the present calculated curves with the curves calculated by Lasaga (1982), both sets of calculated curves are in close agreement for growth in relatively anorthite-rich bulk compositions ($c \geq 0.5$). The primary differences, as expected, are for the more albite-rich compositions. These differences are primarily the result of the higher viscosity values of the Cranmer and Uhlmann (1981) data, as compared to the viscosities calculated after the method of Bottinga and Weill (1972) and Shaw (1972).

Another feature is the discrepancy between the growth-rate curve of Kirkpatrick et al. (1979) and the results of the present study for the An_{20} bulk composition (see Fig. 7). The cause for the discrepancy is uncertain, but may be related to the different experimental techniques employed in the study of Kirkpatrick et al. (1979) and the present study. For large undercoolings, and for all of the experiments with the An_{20} bulk composition, the experiments of Kirkpatrick et al. were carried out with 1-cm^3 glass cubes of the appropriate composition. The experiment consisted of "dusting" the surface of the cube with seed crystals and placing the cube in a 1-atm furnace at the growth temperature. Crystals would nucleate from the seed crystals at the surface of the cube and grow inward from the cube surface. In addition to the possible influence of the cube surface–seed crystal interface on the initiation of growth, another effect is the high amount of crystal impingement that typically occurred in the experiments (see their Fig. 2). Growth experiments with a microscope heating stage were not attempted by Kirkpatrick et al. for the An_{20} bulk composition, as was done for their other compositions, because of the assumed low growth rates (Kirkpatrick, pers. comm.). It should be noted that the results for growth in the An_{40} bulk composition from the present study compare favorably with the results for An_{50} bulk composition of Kirkpatrick et al. (1979). In addition, the results from the present study for the An_{20} bulk composition form an internally consistent data set with the data for the An_{30} and An_{10} bulk compositions.

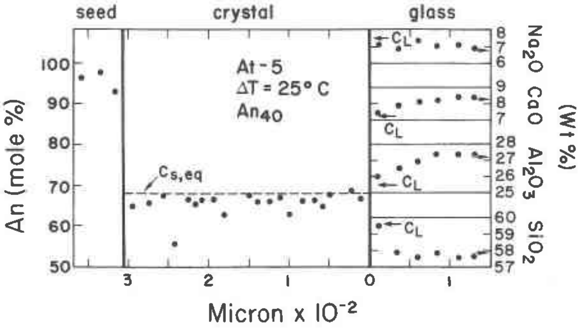

Fig. 11. Compositions of crystal and glass for run At-5.

Compositions of crystals and glass (quenched melt)

Data on compositional zoning in the plagioclase crystals and analyses of concentration gradients in the glass near the crystal-glass interface can provide further insights into the details of the growth process (Lasaga, 1981). In particular, compositional data can be used to evaluate the assumption of local equilibrium at the crystal-melt interface. In addition, compositional data on the crystal provides constraints on possible growth models that involve steady-state (Kirkpatrick et al., 1979; Lasaga, 1981) and nonsteady state conditions (Lasaga, 1982).

Compositional data are provided in Figures 10 and 11 for crystals and glass from two of the 1-atm experiments. At relatively small undercoolings (Fig. 10), the crystal composition is the equilibrium composition for the particular growth temperature. In addition, there are no observed concentration gradients in the glass or the crystal within the precision of the microprobe analyses.

At larger undercoolings in the anhydrous system, the crystal composition corresponds approximately to the equilibrium composition at the particular growth temperature (Fig. 11). Although it was sometimes impossible to analyze the crystals without analyzing glass inclusions or glass that overlapped the crystal, the general trend of the analytical data shows no compositional zoning within the plagioclase crystal. In particular, no evidence was found for oscillatory zoning in *any* of the isothermal experiments.

In contrast to the crystal homogeneity, the glass next to the crystal surface contains concentration gradients for most of the major oxides. The relative widths of the zones containing the concentration gradients for the individual oxides are not equal, which may be related to the effects of multicomponent diffusion. There is a lack of observed concentration gradient of Na_2O, although the analytical precision for Na_2O is substantially less than for the other oxides. As shown in Figure 11, the composition of the glass near the crystal-glass interface is approximately equal to the equilibrium melt composition for the particular temperature of growth, with the exception of the Na_2O content. The change in Na_2O content between the bulk and equilibrium melt compositions is only 1 wt%, however, which is not much greater than the scatter of the analytical data.

CONSTRAINTS ON MODELS FROM COMPOSITIONAL DATA

Small to moderate undercoolings

The lack of observed compositional zoning in the plagioclase crystals and the fact that the crystal compositions are approximately the equilibrium compositions for the growth temperatures place considerable constraints on possible kinetic models. At small to moderate undercoolings, there is the additional consideration that the observed growth-distance curves are linear with respect to time.

At relatively small undercoolings ($\Delta T \leq 20$ deg), no concentration gradients were detected in the glass next to the crystal-glass interface. Thus, growth at relatively small undercooling in the anhydrous plagioclase system would seem to be dominated by an interface-control growth mechanism. The growth rates are sufficiently slow so that diffusive transfer through the melt phase can eliminate concentration gradients in the melt near the crystal-melt interface.

At moderate undercooling ($20 \leq \Delta T \leq 80$ deg), the combination of lack of compositional zoning in the crystals, equilibrium concentrations of solid and glass (melt) phases at the crystal-melt interface, linear growth kinetics, and the presence of concentration gradients in the melt would normally be an argument for the attainment of a steady state during the growth process. A steady state for a system with balanced diffusive and growth mass transfer, however, is only possible if one invokes a model of a chemical boundary layer with convection or hydrodynamic mixing as one of the boundary conditions (Lasaga, 1981, 1982). For the case of moderate undercooling, it appears that either (1) the steady state is controlled by the formation of a diffusive boundary layer, of thickness δ, and convective mixing of melt beyond this boundary layer or (2) the system is not at steady state, but is rather in a slow asymptotic approach to equilibrium. In the case of the latter model, the approach to equilibrium is described by a growth-diffusion equation similar to that derived by Lasaga (1982).

If either model 1 or 2 is operational, the determination of a "true" growth rate that represents growth in the absence of compositional gradients in the melt at moderate to large undercoolings is more involved. Lasaga (1981) has shown that for growth in stagnant boundary layers in stirred systems (model 1), the incorporation of a concentration-dependent growth rate [$Y = f(c)$] can have a substantial effect upon the observed versus "true" growth rate for the system. In particular, there will only be one value of the self-consistent growth rate, Y_{sc}, and one value of $c = C(x = 0)$, the concentration in the melt at the crystal-melt interface, that will satisfy the equation

$$Y_{sc} = f[c(Y_{sc})] \tag{18}$$

and guarantee the attainment of steady state. In order to solve Equation 18, Y is found as a function of melt composition for a particular temperature and the expression for $c(Y)$. For the present example, steady-state growth in the anhydrous bulk composition of $C_{\text{bulk}} = \text{An}_{40}$ at a growth temperature of 1386°C has been chosen; this case is equivalent to the run conditions for the crystal represented in Figure 11. The calculation of Y as a function of composition at 1385°C was simplified by fitting calculated growth rates from Equation 7 to a polynomial in composition

$$\begin{aligned} Y(c) = {} & (8.7418 \times 10^{-3}) + 0.07233X_{\text{An}} \\ & - 0.85497X_{\text{An}}^2 + 3.6523X_{\text{An}}^3 \\ & - 7.0080X_{\text{An}}^4 + 5.1689X_{\text{An}}^5. \quad (\text{cm/min}) \end{aligned} \tag{19}$$

The $c(Y)$ expression is given by

$$C(x = 0) = C_{\text{Bulk}}/[K + (1 - K)\exp(-Y\delta/D)], \tag{20}$$

where K is the partition coefficient ($C_s^{\text{An}}/C_l^{\text{An}}$), δ is the thickness of the chemical boundary layer (cm), and D is the diffusion coefficient (cm²/min). The value of K at the liquidus temperature of the bulk composition (2.15) was used in the calculation. The resulting curve of the self-consistent growth rate and the melt composition at the crystal-melt interface as a function of log (δ/D) is shown in Figure 12. It should be emphasized that the calculated results in Figure 12 are strictly applicable only to growth in the 1-atm plagioclase system; this is because the isothermal experimental growth rates are used as an input parameter. The form of the curve in Figure 12, however, is qualitatively similar to that expected for the general case of crystal growth from multicomponent melts.

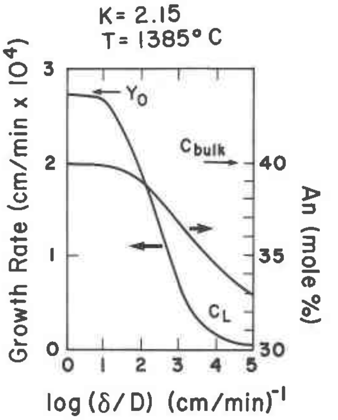

Fig. 12. Plot of self-consistent growth rate and composition of the melt at the crystal-melt interface for various values of δ/D (boundary-layer thickness divided by diffusion coefficient).

One important feature of Figure 12 is the relatively low value for the self-consistent growth rate as the melt composition approaches the equilibrium composition. The model predicts that the true growth rate, Y_0, for the bulk composition would be much greater than the observed growth rate if $\delta/D \gg 1$. The boundary-layer theory, as originally developed by Burton et al. (1953), was formulated for single tracer components, so there is some ambiguity as to choice of the value for δ for the multicomponent system of the present study. For the present discussion, calculations will be performed with the range of δ values observed from the experiments. For a δ of 10^{-3} to 10^{-2} cm (the range of δ values from Fig. 11) and a D of 6×10^{-6} cm²/min (Hofmann, 1980), the appropriate range of log (δ/D) values would be from 2.7 to 3.7. Thus, the actual growth rate for the An_{40} bulk composition in the absence of concentration gradients would be from 2.5 to 15 times larger than the growth rate observed from the experiments at 1385°C. The composition of the melt at the crystal-melt interface for this range of δ/D values is 35 to 38 mol% anorthite. The analyzed glass at the crystal-melt boundary is 36 ± 2.5 mol% anorthite (considering only mole proportions of CaO, Al_2O_3, and SiO_2). The composition of the solid in equilibrium with the melt at the crystal-melt interface, however, is somewhat more albitic than the equilibrium composition (68 mol% An), but is within analytical error (66 ± 2.5 mol%). There is, however, considerable uncertainty concerning the values of D. An increase in D would result in a decrease in the difference between the observed and true growth rates, but would result in a steady-state melt concentration that would be more anorthite-rich, approaching the bulk composition (An_{40}) at low values of δ/D.

A similar discrepancy between the observed and true growth rates at moderate undercoolings results from an analysis of model 2. If Equation 7 is used in conjunction with the growth-diffusion equation of Lasaga (1982), predicted crystal lengths are smaller than the observed lengths from experiments. Such a discrepancy is not entirely unexpected. As in the case of the steady-state model, it is tacitly assumed that the growth-rate equation (Eq. 7) represents growth from the bulk composition with no concentration gradients in the melt near the crystal-melt interface. Because concentration gradients do develop during growth at moderate undercoolings, the observed experimental growth rates do not represent concentration-dependent growth from the bulk composition of the system. In effect, the diffusion-growth equation should be solved for the case of melt convection and development of a stagnant boundary layer. With such an analytical solution, a self-consistent growth-rate formulation could be derived in a manner similar to the steady-state case. Once again, as in the steady-state case, an increase in D would result in a closer fit between the observed and actual growth rates. Another important feature of the analytical solution is that the calculated compositional zoning of a crystal growing at moderate undercooling is steep during the initial stages of growth, but the zoning becomes much less pronounced with time. The plagioclase crystal appears nearly homogeneous except for a thin, relatively steep concentration gradient at the beginning of growth.

Large undercooling

At relatively large undercooling ($\Delta T \geq 80$ deg), crystal lengths achieved during plagioclase growth are not linear functions of time. In this case, the steady-state assumption is not valid; therefore, model 1 would not be applicable. The crystals still appear to be compositionally unzoned when viewed with optical methods, but analysis by microprobe is not possible because of the small sizes of the individual crystals. Either model 2 or a modification of model 2 incorporating disequilibrium partitioning (Hopper and Uhlmann, 1974; Loomis, 1983) could produce the observed nonlinear kinetics.

Although the experimental data presented in this study indicate nonlinear growth rates at large undercoolings for An_{40} and An_{20} bulk compositions (Figs. 5, 6), Kirkpatrick et al. (1979) found linear growth rates at large undercoolings for An_{75} and An_{50} bulk compositions. One possible explanation for the differences is the contrast in viscosity—and therefore, presumably, diffusion rates—between the bulk compositions for equivalent undercoolings. For a ΔT of 200 deg, there is a 10^3 increase in viscosity between the An_{75} and An_{20} bulk compositions. There may be a transition from boundary-layer-controlled, steady-state growth in anorthite-rich melts to diffusion-controlled growth in albite-rich compositions at relatively large undercoolings ($\Delta T > 200$ deg).

Estimation of a pseudobinary diffusion coefficient

If the growth mechanism at moderate undercooling is a steady-state process, a minimum pseudobinary diffusion coefficient can be estimated for albite-anorthite interdiffusion in the melt phase. If steady state is achieved, the thickness of the boundary layer, δ, will be related to the diffusion coefficient, D, and the growth velocity, Y, as $D/Y \geq \delta$ (Lasaga, 1981). For the case of growth in An_{40} melt at 1385°C, the value of δ will be in the range of 30 to 100 μm (see Fig. 10). The appropriate experimental growth rate is 3×10^{-3} cm/min (5×10^{-5} cm/s). A minimum value of D can thus be derived as $D \geq \delta Y$ or $D_{1385°C} \geq 1.5 \times 10^{-7}$ to 5.0×10^{-7} cm²/s. This minimum value of the pseudobinary diffusion coefficient is slightly larger than the value that was employed in the steady-state calculations (10^{-7} cm²/s) and is near the upper limits of measured cation self-diffusion coefficients in natural silicate melts (Hofmann, 1980). It is reassuring that the results of this independent calculation verify the value of D that was initially chosen in a somewhat arbitrary manner. It should be remembered that increasing the value of D will decrease the discrepancy between the true and self-consistent growth rates in the steady-state case and increase the calculated anorthite concentration at the crystal-melt interface.

CONCLUSIONS

Rates have been experimentally determined for crystal growth of plagioclase in anhydrous albite-anorthite melts for the anhydrous bulk compositional range of An_{10}–An_{40}. This study, in combination with the study of Kirkpatrick et al. (1979), has extended the database for anhydrous plagioclase crystallization virtually across the entire binary join. It has been shown that the anhydrous growth-rate curves agree closely to a theoretical extension of a simple, single-component growth theory to multicomponent melt systems. An important aspect of the extension of the simple growth theory is the possibility of predicting crystal-growth rates in multicomponent melt systems from data on single component systems. Agreement between the extension of simple growth theory and experimental data for the H_2O-saturated plagioclase system (Muncill and Lasaga, in prep.) and the haplogranodiorite system (in progress) have been encouraging.

The details of the plagioclase growth mechanism can be constrained by consideration of the multitude of growth models (Lasaga, 1981, 1982; Loomis, 1983). The rate-controlling step at small undercooling appears to be the reaction at the crystal-melt interface. diffusive mass transport, with or without local equilibrium at the crystal-melt interface, is the most likely rate-controlling process at relatively large undercooling. At moderate undercooling, it is not clear whether the growth is controlled by a steady-state process or a slow approach to equilibrium. In a crystal-melt system at steady state at moderate undercooling, however, the composition of the crystal is not the same as that of the melt, which requires advective mass transport in the melt in addition to the diffusive mass transfer (as a consequence of mass balance).

ACKNOWLEDGMENTS

Thanks are due to Gary Lofgren and Norm Gray for thorough and constructive reviews. An earlier version of the manuscript was reviewed by Robert Luth, Bjorn Mysen, and H. S. Yoder, Jr. This research was supported in part by NSF Grant EAR 80-07755 (to Lasaga). Portions of the study represent part of the Ph.D. thesis of Muncill at Pennsylvania State University. Muncill gratefully acknowledges support provided by an AMOCO Graduate Fellowship at Pennsylvania State University. Additional support was provided through the W. M. Keck Foundation research Scholarship at the Geophysical Laboratory.

REFERENCES

Allegre, C.J., Provost, A., and Jaupart, C. (1981) Oscillatory zoning: A pathological case of crystal growth. Nature, 294, 223–228.

Bottinga, Y., and Weill, D. (1972) The viscosity of magmatic silicate liquids: A model for calculation. American Journal of Science, 272, 438–475.

Bottinga, Y., Kudo, A., and Weill, D. (1966) Some observations on oscillatory and crystallization of magmatic plagioclase. American Mineralogist, 51, 792–806.

Bowen, N.L. (1913) The melting phenomena of the plagioclase feldspars. American Journal of Science, 35, 577–599.

Burton, J.A., Prim, R.C., and Slichter, W.P. (1953) The distribution of solute in crystals grown from the melt. Part I. Theoretical. Journal of Chemical Physics, 21, 1987–1991.

Cranmer, D., and Uhlmann, D.R. (1981) Viscosities in the system albite-anorthite. Journal of Geophysical Research, 86, 7951–7956.

Deer, W.A., Howie, R.A., and Zussman, J. (1966) An introduction to the rock-forming minerals. Longman, London, England.

Fenn, P.M. (1977) The nucleation and growth of alkali feldspars from hydrous melts. Canadian Mineralogist, 15, 135–161.

Goodman, A. (1983) Compare: A Fortran IV program for the quantitative comparison of polynomial trend surfaces. Computers & Geosciences, 9, 417–454.

Haase, C.S., Chadam, J., Feinn, D., and Ortoleva, P. (1980) Oscillatory zoning in plagioclase feldspar. Science, 209, 272–274.

Heinrich, E.W. (1965) Microscopic identification of minerals. McGraw-Hill, New York.

Hofmann, A.W. (1980) Diffusion in natural silicate melts: A critical review. In R.B. Hargraves, Ed. Physics of magmatic processes. Princeton University Press, Princeton, New Jersey.

Hopper, R.W., and Uhlmann, D.R. (1974) Solute redistribution during crystallization at constant velocity and constant temperature. Journal of Crystal Growth, 21, 203–213.

Jackson, K.A. (1967) Current concepts in crystal growth from the melt. Progress in Solid State Chemistry, 4, 53–80.

Kirkpatrick, R.J. (1975) Crystal growth from the melt: A review. American Mineralogist, 60, 798–814.

——— (1981) Kinetics of crystallization of igneous rocks. Mineralogical Society of America Reviews in Mineralogy, 8, 321–398.

Kirkpatrick, R.J., Robinson, G.R., and Hays, J.F. (1976) Crystal growth from silicate melts: Anorthite and diopside. Journal of Geophysical Research, 81, 5715–5720.

Kirkpatrick, R.J., Klein, L., Uhlmann, D.R., and Hays, J.F. (1979) Rates and processes of crystal growth in the system anorthite-albite. Journal of Geophysical Research, 84, 3671–3676.

Klein, L., and Uhlmann, D.R. (1974) Crystallization behavior of anorthite. Journal of Geophysical Research, 79, 4869–4874.

Lasaga, A.C. (1981) Implications of a concentration-dependent growth rate on the boundary layer crystal-melt model. Earth and Planetary Science Letters, 56, 429–434.

——— (1982) Toward a master equation in crystal growth. American Journal of Science, 282, 1264–1288.

Loomis, T.P. (1983) Compositional zoning of crystals: A record of growth and reaction history. In S.K. Saxena, Ed. Kinetics and equilibrium in mineral reactions. Springer-Verlag, New York.

Luth, W.C., and Ingamells, C.O. (1965) Gel preparation of starting materials for hydrothermal experimentation. American Mineralogist, 50, 255–259.

Robie, R.A., Hemingway, B.S., and Fisher, J.R. (1978) Thermodynamic properties of minerals. U.S. Geological Survey Bulletin 1452.

Shaw, H.R. (1972) Viscosities of magmatic silicate liquids: An empirical method of prediction. American Journal of Science, 272, 870–893.

Sibley, D.F., Vogel, T.A., Walker, B.M., and Byerly, G. (1976) The origin of oscillatory zoning in plagioclase: A diffusion and growth controlled model. American Journal of Science, 276, 275–284.

Stebbins, J.F., Carmichael, I.S.E., and Weill, D. (1983) The high-temperature liquid and glass heat contents and the heats of fusion of diopside, albite, sanidine and nepheline. American Mineralogist, 68, 717–730.

Swanson, S.E. (1977) Relation of nucleation and crystal-growth rate to the development of granitic textures. American Mineralogist, 62, 966–978.

Turnbull, D., and Cohen, M.H. (1960) Crystallization kinetics and glass formation. In S.D. MackKenzie, Ed. Modern aspects of the vitreous state. Butterworths, London.

Vance, J.A. (1962) Zoning in igneous plagioclase: Normal and oscillatory zoning. American Journal of Science, 260, 746–760.

Winkler, H.G.F. (1947) Kristallgrosse und Abkuhlung. Heidelberger Beitrage zur Mineralogie und Petrographie, 1, 251–268.

MANUSCRIPT RECEIVED MARCH 23, 1986
MANUSCRIPT ACCEPTED NOVEMBER 20, 1986